PRACE INSTYTUTU LOTNICTWA
215, s. 50-59, Warszawa 2011

NUMERICAL STUDY OF HELICOPTER FUSELAGE AERODYNAMIC CHARACTERISTICS WITH INFLUENCE OF MAIN ROTOR

Jerzy Żółtak
Wieńczysław Stalewski
Wiesław Zalewski
Instytut Lotnictwa

Abstract

The influence of simulated main rotor on aerodynamic properties of four different helicopter fuselage configurations has been tested. The research was done using computational fluid dynamics (CFD) method. Simulations were done for hover and forward flight conditions. The results for computation without and with main rotor modelling were compared. Changes of aerodynamic properties with respect to basic configuration were analysed.

1. Introduction

In order to calculate properties of a helicopter, designers are often using aerodynamic characteristics of an isolated helicopter fuselage, obtained by calculation or experimentally. Using this approach it is possible to determine the effect of the various external elements integrated with fuselage [1] on its properties. This approach, however, ignores the impact of the stream generated by the main rotor on fuselage loads.

The paper attempts to evaluate this phenomenon for a light helicopter, using the methods offered by modern CFD technique. Four configurations of helicopter fuselage will be analysed, Figure 1:

- **MB** basic configuration [1] fuselage contains horizontal and vertical tails,
- **MB+2R** configuration **MB** with modified (increased) horizontal tail,
- **MB+W** basic configuration **MB** with additional listing elements (small wing) mounted in central part of the fuselage,
- **MD** alternative geometry [2] of fuselage presented with horizontal and vertical tails

The **MD** configuration was designed to improve aerodynamic parameters of **MB** configuration, particularly to reduce negative lift force in forward flight condition [2]. In Figure 2 the basic differences between **MB** and **MD** are shown.

The analysis will be focused on two aspects in following order:

- influence of simulated main rotor on lift and drag forces and pitching moment distribution on fuselage surface,
- the relative change of forces and moment with respect to **MB** configuration.

The discussion of the result will be preceded with short information about numerical tools used for simulation and description of test conditions.

2. Numerical tests conditions

All numerical simulations were done using FLUENT code [3]. It allows analysis of steady and unsteady flow field around any complex geometry. Motion of flow is described by the Reynolds Averaged Navier-Stokes equations. The finite volume method is used to obtain numerical solution of these equations. Some turbulent models are implemented in the software. A several type of boundary conditions can be used.

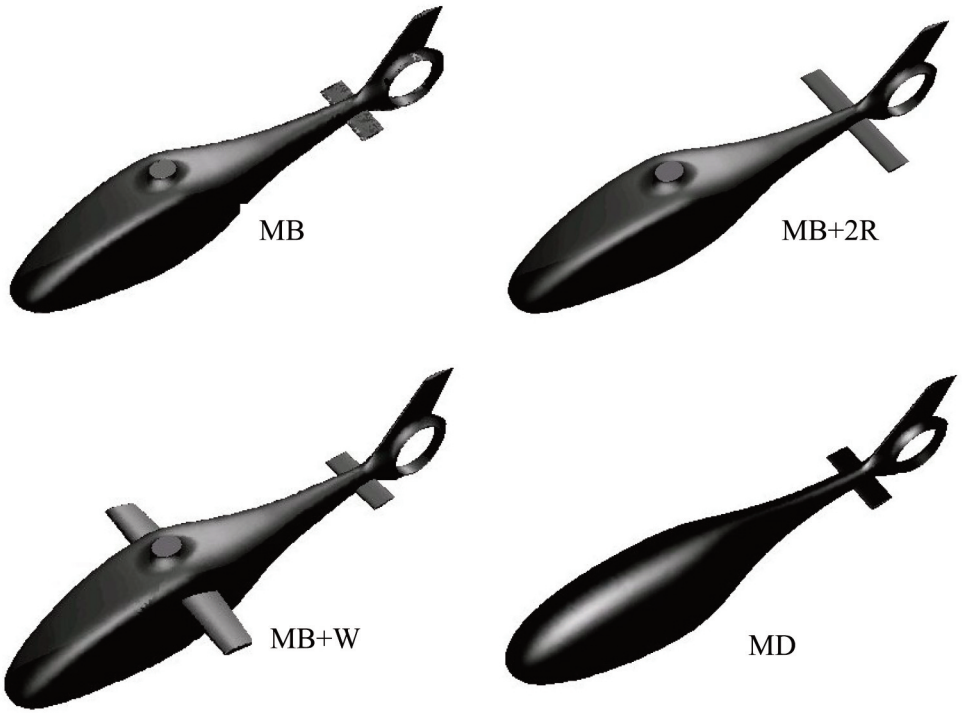

Figure 1. Tested configurations of helicopter fuselage

In the presented analysis following parameters and settings were used:

- 3 dimensional steady calculation
- Spalart – Allmaras turbulent model
- external boundary condition – on all external faces of domain except the backward one (outlet) a pressure far field boundary condition has been set; at outlet a pressure outlet with equal to far field pressure has been used,
- boundary condition at the fuselage – a wall boundary condition.

For simulation of main rotor additional Virtual Blade Model [4] module was used. This module allows for relatively accurate modelling of the rotor influence on fluid avoiding modelling of complete blades, their geometry and movement.
In the method Virtual Blade Model, the rotor is modelled as a layer of cells (Figure 3) with artificial sources of momentum of fluid. The momentum vectors are calculated

based on the aerodynamic characteristics of the airfoils (sections of rotor blades), in accordance with the Blade Element Theory.

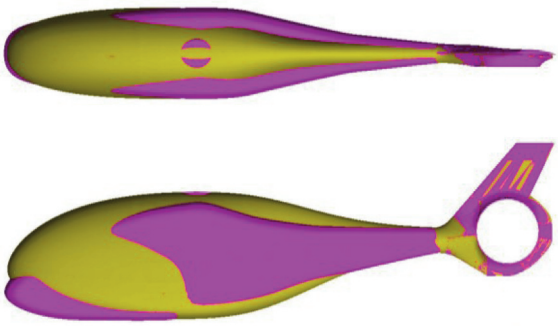

Figure 2. Comparison of the geometry of **MB** and **MD** helicopter fuselage

The mesh for numerical simulation was generated using ICEM CFD [5] software. The typical mesh on fuselage surface and in main rotor domain is presented in Figure 3.

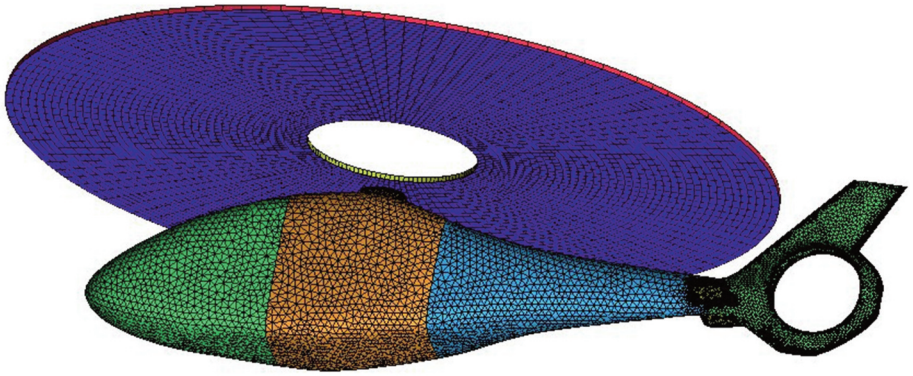

Figure 3. Helicopter fuselage surface and main rotor domain mesh distribution

3. Test conditions

The four configurations of helicopter fuselage presented above with and a configuration without main rotor influence were tested.
In this calculation three-blade rotor based on ILS-2xx airfoils was modelled. The ILS airfoils aerodynamic characteristics database [6], [7], were used to obtain the momentum produced by main rotor. In all simulation the same value of main rotor thrust was assumed. The tests were done for two fight conditions: maximum speed forward flight and hover.

4. Results

In order to make the obtained results more comparable, the geometry of each fuselage was divided into following sections, Figure 4:

- Front fuselage part
- Central fuselage part

- Rear fuselage part
- Vertical tail
- Horizontal tail
- Wing (only for **MB+W** configuration)

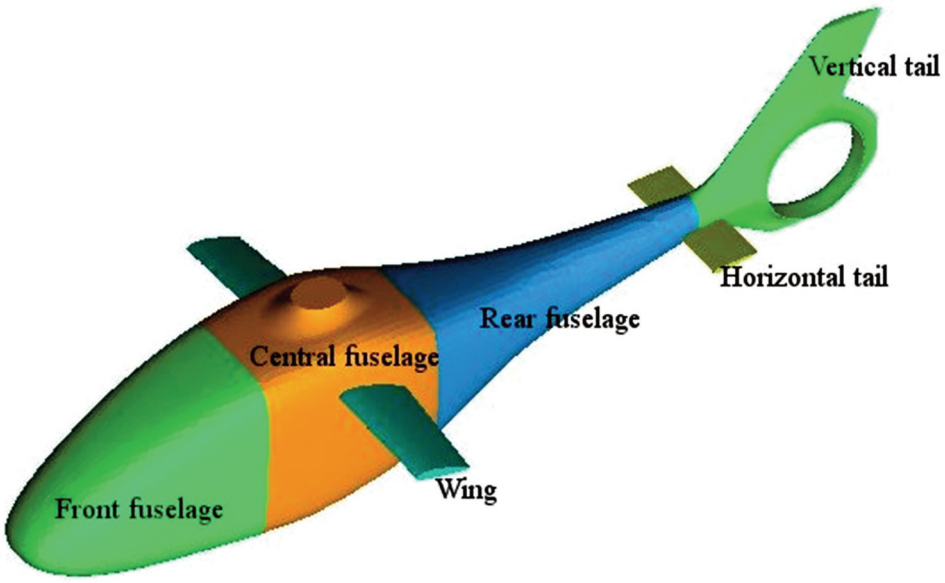

Figure 4. Fuselage's section used in analysis.

For each case of simulation the aerodynamic forces and moments on the fuselage's section were obtained. Basing on these results, additional coefficients were defined for particular analysis. First, to analyse of main rotor influence on aerodynamic forces and moments distribution on the adequate fuselage's sections, the following coefficient was specified:

$$Q_s(Configuration, \sec tion) = \frac{F_s(Configuration, \sec tion)}{\left| F_s(Configuration, total) \right|} * 100$$

where F_S is force or moment calculated based on results of flow field analysed. By definition, the coefficient Q_S saves the direction of aerodynamic force and sign of pitching moment.

The results for configurations: **MB**, **MB+2R**, **MB+W** and **MD**, with and without simulation of main rotor influence, were compared respectively in Table 1, Table 2, Table 3 and Table 4.

In the tables the background of cells with positive value of coefficient has been set to gray. This way it is easier to notice, that the main rotor does not change the qualitative image of forces and pitching moment coefficient distribution on analysed segments of the fuselage.

MB	without main rotor			with main rotor		
	Q_X	Q_Z	Q_{MY}	Q_X	Q_Z	Q_{MY}
centre fuselage	26,5	42,7	-39,3	21,5	41,6	-41,2
rear fuselage	-10,8	6,3	-4,8	-14,0	10,7	-7,7
front fuselage	24,7	-105,5	-318,3	39,7	-104,6	-388,3
vertical tail	52,8	-2,8	55,9	46,3	-2,5	58,7
horizontal tail	6,9	-40,7	206,4	6,5	-45,2	278,5
total	100,0	-100,0	-100,0	100,0	-100,0	-100,0

Table 1. Comparison of forces and moment section distribution for **MB** configuration without and with simulation of main rotor

MB + 2R	without main rotor			with main rotor		
	Q_X	Q_Z	Q_{MY}	Q_X	Q_Z	Q_{MY}
centre fuselage part	22,6	19,6	-8,6	19,5	18,2	-7,0
rear fuselage part	-6,9	2,2	1,9	-9,9	2,8	2,4
front fuselage part	21,8	-51,0	-73,0	35,4	-47,9	-63,5
vertical tail	47,4	-2,5	16,1	42,3	-2,5	13,3
horizontal tail	15,2	-68,2	163,6	12,7	-70,6	154,8
total	100,0	-100,0	-100,0	100,0	-100,0	-100,0

Table 2. Comparison of forces and moment section distribution for **MB+2R** configuration without and with simulation of main rotor

MB + W	without main rotor			with main rotor		
	Q_X	Q_Z	Q_{MY}	Q_X	Q_Z	Q_{MY}
centre fuselage	21,9	635,7	-41,2	19,3	99,8	-38,7
rear fuselage	-10,4	207,0	-25,8	-13,4	29,2	-20,5
front fuselage	24,8	-1170,9	-327,1	36,7	-200,4	-337,7
vertical tail	42,0	-56,7	66,4	38,5	-5,8	52,2
horizontal tail	8,0	-497,9	232,4	8,0	-89,9	251,8
Wing	13,8	782,9	-4,8	10,9	67,0	-7,1
Total	100,0	-100,0	-100,0	100,0	-100,0	-100,0

Table 3. Comparison of forces and moment section distribution for **MB+W** configuration without and with simulation of main rotor

MD	without main rotor			with main rotor		
	Q_X	Q_Z	Q_{MY}	Q_X	Q_Z	Q_{MY}
centre fuselage	44,0	26,2	-19,0	31,7	36,6	-22,8
rear fuselage	-27,0	15,1	5,0	-29,0	17,5	5,7
front fuselage	6,7	-73,5	-117,0	30,8	-84,3	-174,5
vertical tail	64,8	-7,7	52,9	53,7	-7,2	59,6
horizontal tail	11,5	-60,1	178,0	12,9	-62,6	232,0
total	100,0	-100,0	100,0	100,0	-100,0	100,0

Table 4. Comparison of forces and moment section distribution for **MD** configuration without and with simulation of main rotor

For all configurations the total value of Q_Z for cases without and with main rotor is negative. It denotes, that on fuselage the negative lift force is generated. A value of total Q_{MY} shows, that for configurations **MB**, **MB+2R** and **MB+W** pitching moment pushes down the fuselage's nose. The situation for **MD** configuration is different – pitching moment lifts up the nose of fuselage.

In next step the relative changes of drag and lift forces and pitching moment with respect to **MB** configuration is analysed. This analysis is limited to results of simulation with modelling of working main rotor. In this case the following coefficient was defined:

$$\Delta_S(Configuration, section) = \frac{F_S(Configuration, section) - F_S(MB, section)}{\left|F_S(MB, total)\right|} * 100$$

where F_S is calculated for analysed flow field drag, lift and pitching moment respectively.

HOVER	MB		MB+2R – MB		MB+W – MB		MD – MB	
	Q_Z	Q_{MY}	Δ_Z	Δ_{MY}	Δ_Z	Δ_{MY}	Δ_Z	Δ_{MY}
centre fuselage	-10,1	-7,7	10,2	1,0	0,0	17,3	7,1	8,9
rear fuselage	-36,5	352,6	3,7	-12,3	0,0	29,1	21,7	-207,3
front fuselage	-46,6	-346,6	1,4	35,9	0,0	31,0	2,1	30,3
vertical tail	2,2	-50,9	1,0	-26,1	0,0	3,2	0,1	-3,1
horizontal tail	-9,0	152,6	2,1	-24,6	0,1	-136,7	4,2	-63,2
wing	0,0	0,0	0,0	0,0	-30,2	167,8	0,0	0,0
total	**-100,0**	**100,0**	**18,4**	**-26,0**	**-30,1**	**111,9**	**35,1**	**-234,4**

Table 5. Comparison of lift force and pitching moment with simulation of main rotor for tested configurations in hover

Δ_Z	MB+2R – MB	MB+W – MB	MD – MB
centre fuselage	-1,6	11,2	-13,2
rear fuselage	-4,7	4,7	2,9
front fuselage	-0,6	-1,5	39,0
vertical tail	-3,0	-0,6	-3,1
horizontal tail	-109,7	-2,4	-3,5
wing	0,0	35,5	0,0
total	-119,6	47,0	22,1

Table 6. Comparison of lift force with simulation of main rotor for tested configuration for forward flight

From definition the positive value of defined above coefficient denotes in case of :

- Δ_Z that negative value of lift is reduced (positive phenomena)
- Δ_X that value of drag is increased (negative phenomena)
- Δ_{MY} that negative value of pitching moment is reduced

In Table 5 the results of hover condition tests are collected. It can be seen that configurations **MB+2R** and **MD** reduce the negative value of lift with respect to **MB** configuration. Quite different situation is observed for **MB+W** - the additional negative lift is generated on wing.

Δ_X	**MB+2R – MB**	**MB+W – MB**	**MD – MB**
centre fuselage	0,4	1,2	3,8
rear fuselage	2,9	-1,8	-9,1
front fuselage	0,0	3,3	-15,2
vertical tail	1,2	-1,1	-3,5
horizontal tail	7,7	2,9	3,8
wing	0,0	12,9	0,0
total	12,2	17,4	-20,3

Table 7. Comparison of force with simulation of main rotor for tested configuration for forward flight

The positive value of pitching moment, which characterizes the **MB** configuration, is reduced for both above configurations. For **MB+2R** this reduction is equal approximately 75%. For **MD** configuration reduction is so large, that radically changes the property of the fuselage. The fuselage's nose moves down instead being lifted up.

The results for forward flight are presented in Table 6, Table 7 and Table 8. In Table 5 the lift coefficients are compared. The influence of lift force generated on horizontal tail in **MB+2R** configuration (negative value) and wing in **MB+W** configuration (positive value) on total value of coefficient Δ_Z for this both configurations is easy to observe.

Finally for **MB+2R** configuration the negative value of lift is decreased (value of lift increases). Lift is also increased by a little more than 50% for **MB+W** configuration. The reduction of negative lift is also noticed for **MD** configuration, but it is smaller than characterized **MB+W** configuration. It is important to note that this reduction was achieved by substantial redistribution of lift between fuselage components/sections: on central part of fuselage the negative value of lift increases, on front/nose part of fuselage the significant reduction of negative lift is observable.

It is interesting how the above discussed changes in the lift force correlating with the changes of the drag force. In Table 7 the values of Δ_X were collected. From this comparison one can see, that for **MB+2R** and **MB+W** increases of the drag, relate to **MB** configuration, are approximately 12 and 17 units respectively. The main part of drag increment for **MB+2R** configuration is produced by horizontal tail. For **MB+W** configuration additional drag is generated by the wing. Only for **MD** configuration the reduction of drag is observed - the value of Δ_X decreases approximately 20 units. In this case, total value of Δ_X is strongly dependent on two components: front (nose) and rear part of fuselage. The contributions of both parts are approximately equal -24 units.

In Table 8 the values of Δ_{MY} for tested configuration are presented. For **MB+W** configuration the increase of pitching moment negative value is observed.

Δ_{MY}	MB+2R – MB	MB+W – MB	MD – MB
centre fuselage	-1,8	-4,1	11,5
rear fuselage	22,5	-16,3	15,1
front fuselage	-1,5	-7,2	160,9
vertical tail	22,9	2,4	19,0
horizontal tail	671,5	16,4	23,9
wing	0,0	-8,3	0,0
total	713,6	-17,1	230,3

Table 8. Comparison of pitching moment with simulation of main rotor for tested configuration for forward flight

The pitching moment properties of both other configurations: **MB+2R** and **MD** are completely different. They are characterized by positive value of pitching moment (the change of Δ_{MY} is greater than 100 units). Main influence on this change has the pitching moment generated on horizontal tail (approximately 671 units) and front (nose) fuselage part (approximately 160 units) for **MB+2R** and **MD** configuration respectively.

5. Conclusions

In the paper the influence of main rotor on aerodynamic parameters for different configurations has been tested. The research was done using computational fluid dynamics (CFD) method. The four geometries were briefly presented. First three (**MB**, **MB+2R**, **MB+W**) are having the same fuselage concept with different configurations of external elements. The last fuselage (**MD**) was numerically designed for the same flight conditions as base configuration to improve its properties. Next the numerical tools (FLUENT and VBM model) were shortly presented.

At the beginning the influence of main rotor modelling on force and moment distribution on fuselage was tested. In this case the simulations for forward flight conditions were done for all fuselage configurations without and with main rotor. The results of calculations show, that the main rotor does not change the qualitative image of forces and pitching moment coefficient distribution on analysed components of all fuselage configuration.

Next the change of forces and pitching moment of **MB+2R**, **MB+W**, **MD** configuration with respect of **MB** configuration properties was analysed. For this case calculations were done for hover and forward flight conditions. Basing on results of these simulations the following conclusion can be formulated:

- For hover condition the configuration **MB+2R** and **MD** reduces the negative value of force and changes the sign of pitching moment from positive to negative, at the same time change is greater for the **MD** configurations.

- The **MD+W** configuration in hover has similar properties as **MB** configuration, but it achieves greater values of negative lift force and positive pitching moment compared to base configuration.
- For forward flight for configurations **MB+W** and **MD** the reduction of negative lift force can be observed
- Only configuration **MD** reduces the drag force
- Similar as in hover, for forward flight the **MB**+R and **MD** configurations, in respect to **MB** configuration, changing the sign of pitching moment, but in this case the change is from negative to positive value.

Above discussion leads to conclusion that **MD** configuration of fuselage shows the way, how to change existing geometry in order to obtain better aerodynamic characteristics.

6. Bibliography

[1] Grzeorczyk K., Dziubiński A., Numerical analysis the influence of the light helicopter's external components on the aerodynamic characteristics, Transaction of Institute of the Aviation (in print)
[2] Stalewski W., Żółtak J., Multi-Criteria Design and Optimisation of Helicopter Fuselage, in Evolutionary and Deterministic Methods for Design, Optimization and Control with Applications Industrial and Societal Problems, Eds: Poloni C., Quagliarella D. at all, © CIMNE, Barcelona, Spain 2011 (in print)
[3] FLUENT, http://www.ansys.com
[4] http://www.fluvius.com.au/FLUENT_UGM05/UGM05_Virtual_Blade_Model_VBM.pdf
[5] ICEM CFD, http://www.ansys.com
[6] Instytut Lotnictwa Internal Report No. 115/BA/95/D.
[7] Instytut Lotnictwa Internal Report No. 117/BA/95/D.

Acknowledgments

This research was supported by project No. O R00 0048 08 founded by Ministry of Science and Higher Education.

Jerzy Żółtak. Wieńczysław Stalewski, Wiesław Zalewski

NUMERYCZNE STADIUM WPŁYWU MODELOWANIA WIRNIKA NOŚNEGO NA CHARAKTERYSTYKI AERODYNAMICZNE KADŁUBA ŚMIGŁOWCA

Streszczenie

Wpływ symulacji wirnika głównego na własności aerodynamiczne czterech różnych konfiguracji kadłuba śmigłowca został przebadany. Badania obliczeniowe przeprowadzono wykorzystując metody numerycznej mechaniki płynów. Obliczenia wykonano dla zawisu oraz lotu postępowego. Porównano wyniki uzyskane bez i z symulacją wpływu wirnika nośnego. Analizowano również zmianę własności aerodynamicznych badanych konfiguracji względem konfiguracji bazowej.